LA-UR- 95-2674

Title: POSSIBILITIES FOR MAGNETIC CONTROL OF FISSION PLASMA PROPULSION

Author(s): R. A. Gerwin, R. A. Nebel, Theoretical Division, T-15
D. I. Poston, TSA-12
Los Alamos National Laboratory

Submitted to: 31ST AIAA/ASME/SAE/ASEE JOINT PROPULSION CONFERENCE AND EXHIBIT, JULY 10-12, 1995/San Diego, CA

DISTRIBUTION OF THIS DOCUMENT IS UNLIMITED

MASTER

Los Alamos
NATIONAL LABORATORY

Form No. 836 R5
ST 2629 10/91

AIAA 95 - 2903

Possibilities for Magnetic Control of Fission Plasma Propulsion

R. A. Gerwin, D. I. Poston, and R. A. Nebel
Los Alamos National Laboratory
Los Alamos, NM

31st AIAA/ASME/SAE/ASEE
Joint Propulsion Conference and Exhibit
July 10-12, 1995/San Diego, CA

Possibilities for Magnetic Control of Fission Plasma Propulsion

R. A. Gerwin*, D. I. Poston**, and R. A. Nebel*
Los Alamos National Laboratory, Los Alamos, New Mexico

Abstract

Magnetic fusion energy research suggests the use of some magnetoplasma configurations to address certain critical issues in the gas-core fission approach to nuclear-thermal propulsion. The general framework of such an investigation that was outlined in a previous paper is directed here at the spheromak configuration in greater detail. In some unoptimized examples, we explore the compatibility of gas-core fission reactor criticality conditions with the dynamo action needed to non-inductively sustain the spheromak. The Lundquist number S is identified as a figure of merit, and is estimated by modeling to be as large as 100 in near-critical uranium (^{233}U) plasmas of several-meter dimensions diluted with lithium (^{7}Li) when the spheromak power consumption is treated as a constraint; whereas S as small as 200 is observed to be still able to preserve MHD dynamo activity in 3D resistive MHD simulations. Further optimization studies are required to ascertain whether these two values can be made to coincide.

Introduction

The gas-core fission approach to nuclear thermal propulsion has long attracted interest because the absence of solid structures within the reactor (fuel rods and heat transfer walls) allows higher temperature operation, and concomitantly increased specific impulse from the heated propellant in an inherently high thrust device.[1-4] The simplest version of this approach to nuclear-thermal propulsion is illustrated in Fig. 1-a. However, comprehensive self-consistent simulations[1] indicated that ideally separate fuel and propellant volumes are subject to dynamical mixing, thereby impeding the smooth flow of propellant to the nozzle and diluting and cooling the fissionable fuel core. Moreover, even a slight rocket acceleration was found to cause the fuel to displace the propellant in the neighborhood of the nozzle, leading to a rapid loss of fuel and a global deterioration of the propellant flow field.

To address these critical issues, a general framework has been outlined for exploring the feasibility of magnetic control of gas-core fission plasmas (the fuel) by means of the simplest steady state configurations, namely, magnetic mirrors and spheromaks.[5] Theoretical indications were there provided to the effect that magnetic fields can stiffen the fuel-propellant interface against Kelvin - Helmholtz type instabilities, and that, for magnetic mirrors in compact systems, bad-curvature regions that drive Rayleigh - Taylor type instabilities need not occur. Magnetic pressure balance of the core plasma is not feasible for these highly resistive high-pressure plasmas, which must be contained by the propellant or the wall; nevertheless, active magnetic guiding of the plasma-fuel flow was shown to be feasible for moderate field strengths of order 0.1 T, even in highly resistive uranium plasmas of a few eV temperature and including the effect of rocket accelerations of order g_0. Magnetic guiding can be resistively effected by the cross-field-flow-induced generation of a magnetic body force in the direction opposite to that flow. Active magnetic guiding of deliberately generated parallel flow of the fuel provides a lever with which to mitigate un-controlled fuel-propellant dynamical mixing, for instance if each species were to have its own nozzle, one on axis and one annular; but then magnetic deflection would have to be invoked to recycle the fuel. Assuming that the fuel leaves through a nozzle with choked flow, an example was presented for which a nozzle area ratio to the main reactor chamber of 10^{-3} implied a magnetic field in the nozzle throat near one megagauss (much more than is needed for magnetic deflection but which is required by the magnetic mirror geometry), as well as the necessity to magnetically recycle several kg/s of fuel. Here, a reduction in the recycling rate by the utilization of thinner nozzles implies the occurrence of multi-megagauss fields in the mirror-nozzle throat.

In contrast, a spheromak concept also was suggested there,[5] which does not envision a primary outflow of fuel through a nozzle. Instead, it was pointed out that cross-field flow of plasma is subject to a resistive

---

Presented as paper AIAA-95-2903 at the 31st AIAA/ASME/SAE/ASEE Joint Propulsion Conference, July 10-12, 1995, San Diego, CA.

* Staff Member, Theory Division
** Staff Member, Technology and Safety Assesment Division

friction (as described above), leading to the idea of pellet injection of fuel into the toroidal core of the spheromak, with enhanced retention of ionized fuel in the core due to this resistive friction. A schematic diagram of this approach to nuclear-thermal propulsion is displayed in Fig. 1-b. A characteristic slowing-down time for the cross-field flow of resistive plasma was identified and estimated to be quite short and therefore presumably quite effective in retaining the plasma. Of course, gradual depletion of the core and recycling of the fuel ultimately would then have to be dealt with, but apparently at a much lower rate than that associated with the magnetic mirror approach. (This optimistic prospect must be subject to re-examination and possible concept modification in view of the dynamo activity that is needed to non-inductively sustain the spheromak, as discussed below.)

A critical issue for the spheromak approach is its non-inductive sustainment under conditions required for fission-reactor criticality. This type of sustainment involves the injection of magnetic helicity along the open magnetic field lines, and is thought to be mediated by the excitation and saturation of global magnetohydrodynamic symmetry-breaking instabilities.[6,7] The presence of plasma resistivity, no matter how small, allows the MHD instabilities to cause changes of magnetic field line topology necessary to access states of lower magnetic energy.[8] However, resistivity also produces resistive diffusion of the MHD mode structures, weakening their activity; and resistivity is also responsible for unwanted evolution of the mean axisymmetric equilibrium state of the plasma. (Since there can be no steadily applied voltage along the toroidal magnetic axis of the spheromak, its pure axisymmetric embodiment would necessarily decay away in the absence of any other effects.) The latter is combatted by axisymmetric contributions to the Lorentz electric field from second-order products of non-symmetric MHD fluctuations, and this is known as sustainment by the dynamo effect.[9]

The competition between the time scale for MHD activity (nominally a radial Alfven time, r/V_A) and a nominal resistive diffusion time scale, r^2/D, where D is the resistive diffusivity η / μ_0, is characterized by the ratio of the latter time to the former. This leads to the Lundquist number, $S = rV_A/D$, which is like a magnetic Reynolds number but with the plasma flow velocity replaced by the Alfven velocity. In magnetic fusion energy research, one generally is interested in very large values of S, 10^6-10^8, and even higher values. In the case of interest here, however, our concern is that S will be so small as a result of the high plasma resistivity that MHD instabilities will be resistively damped, to the point that they cannot contribute to the dynamo activity needed to counter the rapid resistive decay of the spheromak configuration. In this paper, we shall estimate values of S obtainable from non-optimized examples of gas-core fission propulsion configurations, and shall compare them to the lowest S value observed to produce dynamo sustainment in a non-optimized three-dimensional resistive MHD simulation.

Approximate Estimates of Gas-Core Fission Parameters

In this section, we shall discuss order-of-magnitude estimates of gas-core fission reactor parameters, and in the following section shall present quantitative numerical results from detailed computational models. The approximate estimates serve to provide some insight into the magnitudes and scalings obtained by the computerized models.

Reactor Size and Gas-Core Number Density for Criticality

In ref. (5), a spherical gas core of ^{235}U was considered, surrounded by a thick neutron moderator-reflector material such as beryllium oxide. Fast neutrons (energies of order 1 MeV), originating from fission events in the core, enter the reflector material, are slowed to thermal energies, and eventually are scattered back into the core as thermal neutrons where they induce more fissions. A simple two-energy-group diffusion model was applied to the neutrons, which immediately led to a concise criticality condition for a steady state reactor. Plots of this condition are in terms of number density of fissionable atoms vs reactor size (core radius). From such plots, one concludes that compact (meter-size) gas-core fission reactors require atmospheric- type number densities ($\sim 10^{19}$ cm^{-3}) of ^{235}U. This feature is a direct consequence of the size of the thermal-neutron fission cross section of ^{235}U.

These plots also showed that there is approximately a reciprocal relation between number density and core size. This feature can be understood from the standpoint that criticality requires approximately a fixed ratio of slow-neutron fission mean free path to core size. The presence of a thick layer of reflector material allows multiple passes of slow neutrons through the core, so that the fission mean free path can somewhat exceed the core size of a steady state reactor that utilizes a thick reflector.

Reactor Power Level and Gas-Core Temperature

The power level at which the reactor operates depends upon its start-up history, and is independent of the conditions required for criticality. If the core residence time is long enough (which it easily is), then the final steady-state core temperature basically is a consequence of the balance between fission power production and heat transfer to external materials such as the propellant and the walls and wall-coolant of the vessel. In the situation of interest to us here, the core temperature acquires additional significance in that it determines the electrical resistivity of the core plasma and concomitantly the capacity of the plasma to be influenced by magnetic fields. In our computational modeling, it was noticed that the core temperature is not strongly dependent upon the power level of the reactor.

A simple model of this power balance can be constructed for a cylindrical vessel, wherein fission power is generated uniformly within the vessel and heat is transported radially outwards as thermal radiation through a highly opaque medium.[10] Dependence on axial coordinate is neglected, as is the heat loss to the ends of the cylinder. Thus

$$p_f = \nabla \cdot q \tag{1}$$

where p_f is the fission power density and q is the heat flux vector. One expresses the heat flux in terms of the temperature gradient as

$$q = -\kappa \nabla T \tag{2}$$

where κ is the thermal conductivity of the highly opaque medium and T is the local temperature of the medium (the core plasma). Considering an arbitrary internal surface receiving black body radiation from surfaces one photon mean free path to either side, one can calculate the differential net heat flux toward the cooler surface and thereby find the thermal conductivity as

$$\kappa = \frac{16}{3} \frac{\sigma_{SB}}{A_{Ross}} T^3 \tag{3}$$

wherein σ_{SB} is the Stefan - Boltzmann constant and A_{Ross} is the Rosseland-mean absorption constant, which also constitutes the reciprocal of the effective photon mean free path. (The factor 16/3 is due, in part, to integration over the angular distribution of radiation from each surface element.) Finally (see Fig. 2), one can plot on log-log paper the temperature dependence of A_{Ross} from available tables for uranium plasma,[10] and one then finds (for a pressure of 1000 atm) that, to high accuracy between 1 eV and 10 eV, A_{Ross} obeys a power law.

$$A_{Ross} = A_0 T^{-\beta} \tag{4}$$

Here, the temperature is in degrees K, the exponent is $\beta = 2.4$, and the prefactor is $A_0 = 6.2\ 10^{15}\ K^{2.4}\ m^{-1}$. Combining Eqs. (1)-(4), one then obtains an analytic solution for the radial temperature profile, from which one also can extract an expression for the central temperature of the core, T_0. One thereby finds

$$T_0 = \left\{ 0.3 \frac{A_0}{\sigma_{SB}} p_f R^2 \right\}^{1/6.4} \qquad (5$$

where R is the wall radius. Thus, the transport process for thermal radiation through a highly opaque plasma, and the temperature dependence of the plasma opacity, jointly produce a core temperature that does not depend strongly on size, on power density (hence on total power), and on the number density of atoms producing the opacity (through A_0). The central temperature T_0 from Eq. (5) is about 74000 K for 10 GW of fission power in a cylinder of length 6 meters and radius 4 meters containing a uranium number density of about $2\ 10^{19}\ cm^{-3}$, which result is quite close to the more detailed computational result. Moreover, the analytical scaling is meaningful, producing a ten percent drop in temperature from halving A_0, and a thirty percent drop from decreasing A_0 by ninety percent. both results of which are in excellent agreement with the computational heat transfer model described below.

Computational Model Results for Gas-Core Fission Parameters

In this section, computational models are used to estimate neutronic, thermal, and thruster characteristics of the gas core reactor, assuming that magnetic control is indeed successful in maintaining a stable fuel-propellant configuration such as shown schematically in Fig. 1. Then, reversing our viewpoint in a later section, we shall utilize the resulting plasma parameters to estimate the feasibility of magnetic control within the context of the spheromak configuration. (A totally self-consistent computational model including neutronics, thermal hydraulics, and MHD effects does not yet exist.)

Neutronic Analysis

We wish to consider somewhat lower core densities and somewhat larger reactor sizes than studied earlier[1], because these modifications will serve to enlarge the Lundquist number described in the Introduction. Moreover, the reciprocal relation mentioned above between core density and reactor size dictates that larger size is needed to maintain criticality at lower core densities. Supposing that the number density of fissionable uranium atoms is $1.0\ 10^{18}\ cm^{-3}$, then criticality can be achieved in meter-size systems that are only moderately larger in linear dimensions than those considered previously,[1] due to the utilization here of ^{233}U instead of ^{235}U together with the deployment of thicker layers of moderator and propellant.

A simple MCNP model[11] was generated for a cylindrical system with radius 4 meters, length 6 meters, surrounded by a wall layer 0.6 meters thick of BeO on all sides. Assuming the uranium core temperature to be 7 eV and the hydrogen propellant to be at 2 eV, the behavior of thermal neutrons and consequent reactor criticality were computed. When hydrogen is this hot, it constitutes a poison to the nuclear chain reaction with ^{235}U due to energy upscattering of the thermal neutrons by the propellant. As thermal neutrons move from the reflector/moderator to the fuel, they upscatter to energies of 1 - 2 eV. This makes criticality very hard to achieve for isotopes that have most or all of their fission resonances in the thermal range. For this reason, ^{233}U is generally the best fuel for gas core reactors because of its relatively large fission cross section in the 1 - 2 eV range. Thus, ^{233}U results in a criticality parameter k_{∞} being 20% - 40% higher than for ^{235}U (depending on the hydrogen layer thickness), and higher than ^{239}Pu as well.

Because of the hydrogen's negative effect on criticality, the thicker the hydrogen layer between the reflector and the fuel the lower the resulting k_{∞}. In terms of heat transfer, however, a thicker (seeded) hydrogen layer results in a lower wall heat flux and/or a higher propellant exit temperature into the nozzle. Thus, the neutronic analysis can be used to help determine the optimal propellant layer thickness within the context of a reactor-thruster system. For ^{233}U, the hydrogen layer has a negative worth of about 0.5% Δk_{∞} per

centimeter of hydrogen, compared to 1.5% for ^{235}U. For a reactor with the given dimensions, a 30 cm layer of hydrogen surrounding a ^{233}U core of the given density yields $k_{eff} = 1.05$.

As mentioned earlier, the core opacity is smaller at reduced densities of the uranium atoms producing the opacity, leading to reductions in core temperature. Therefore, higher uranium core densities than 10^{18} cm^{-3} could be of interest. In any case, for moderately lower core densities and temperatures, or higher densities and temperatures, the criticality condition ($k_{eff} = 1.0$) can easily be retained by adjusting the thicknesses of the hydrogen layer and of the neutron reflector. (For somewhat thinner hydrogen layers with other conditions as stated, we had already found $k_{eff} > 1.1$.)

Under the conditions of interest, the average charge state of uranium ions is substantially larger than unity,[5,10] in fact Z = 3 - 4. The correspondingly enlarged Coulomb scattering cross section of the ions constitutes a principal impediment to the attainment of high electrical conductivity and high Lundquist number. This situation motivated our exploration of adding a low-Z element to the core so as to reduce the average ionic charge state. As one possibility (but not the only one), we considered ^{7}Li. This substance proves to have very little effect on the opacity, which is primarily due to uranium.[12] It also proves to have very little effect on k_{eff} (provided that it is not contaminated with ^{6}Li), even if the lithium number density exceeds that of the uranium by more than an order of magnitude. Finally, replacement of some uranium with lithium reduces the mass density of the core, and thereby increases the Alfven velocity and hence the Lundquist number.

Heat Transfer Analysis

To estimate the rocket performance, a heat transfer solution is obtained by means of the computer code DIP.[1] It is assumed that the fuel and the propellant do not mix because of the presence of the magnetic field, that the propellant mass flow rate is 100 times greater than that of the fuel, and that the fission power density is uniform within the fuel region. The configuration is similar to Fig. 1-a. Just as for the neutronic solution, the hydrogen layer thickness is the key parameter for the heat transfer solution. A thicker layer has a positive influence on the heat transfer solution, whereas it has a negative effect on the neutronic solution.

The effect of thickening the hydrogen layer depends on the ratio of total fission power to hydrogen mass flow rate, P_f/H_{flow}, where $H_{flow} = \dot{m}_{prop}$. If this ratio is relatively small, then a thicker hydrogen layer results in a lower wall heat flux because heat from the fuel takes longer to propagate toward the wall as the flow moves downstream. Since the limiting factor of the specific impulse is usually the wall heat flux, then a thicker hydrogen layer will allow a larger power and thus a larger I_{sp}. On the other hand, if P_f/H_{flow} is large (which is the case in this system unless extremely large thrusts are desired) then a thicker hydrogen layer results in a higher propellant exit temperature at the nozzle entrance. In this case, the hydrogen becomes saturated with heat near the exit (reaching a constant temperature profile), such that all of the power generated in the fuel is transferred to the wall. Thus, the wall heat flux is limited by the ratio of the power to the radial heat transfer area. As a result, the radial hydrogen temperature profile is fixed by this wall heat flux. A thicker hydrogen layer utilizes more of the high temperature region of this profile, resulting in a higher average propellant exit temperature at the nozzle entrance, and thus again a higher I_{sp}.

The core-exit hydrogen temperature at the entrance to the nozzle, for a 10 GW reactor with a 10 kg/s propellant flow rate and a 30 cm thick hydrogen layer at the wall, proves to be 14400 K, resulting in a specific impulse of 2800 s and a thrust of 280 kN. The associated maximum wall heat flux is 60 MW/m^2. Doubling the propellant flow rate proves to increase the thrust to 500 kN and reduces the wall heat flux to 30 MW/m^2, but the I_{sp} then drops to 2550 s. These latter numbers imply that an initial vehicle mass of 1000 tonnes can receive a mission Δv of 10^4 m/s in about 4 1/2 hours while expelling about 330 tonnes of propellant.

Other results obtained from the computational modeling are as follows. The peak core temperatures obtained by artificially varying the specific heat of the core substance were practically independent of this variation because the core always heated up within very short travel distances (compared to vessel length)

from the entrance port, an effect which also was verified by simple modeling. (This result suggests that diluting the core with lithium should not appreciably influence the core temperature except for the reduced opacity resulting from the reduced number density of uranium ions.) The Rosseland-mean absorption constant corresponding to a uranium number density of about 2 10^{19} cm^{-3} produced a fuel temperature of 67652 K; and, replacing this absorption constant by one half, one quarter, and one tenth of its original value (as induced by corresponding reductions in the uranium number density) produced fuel temperatures of 60310 K, 53810 K, and 46110 K, respectively, in excellent agreement with the scaling from Eq. (5). In all of these cases, the heating of the propellant and the heat transfer to the wall remained practically unchanged.

Magnetic Manipulation of the Plasma Core

In this section, we explore the notion of magnetic field interactions for plasmas having the kinds of parameters described above, with emphasis on the spheromak. We begin by presenting some three dimensional resistive MHD simulation results, explaining their relevance, and pushing the parameters to see what happens to highly resistive plasmas. The question is one of the extent to which uranium plasma interactions with magnetic fields in the form of growth and saturation of MHD modes continue to constitute important processes as the Lundquist number is reduced. We then estimate some Lundquist numbers that correspond to the fission core plasmas discussed earlier, and compare them to those of the MHD simulations.

Discussion of MHD Simulations

Three dimensional resistive MHD simulations of *non-inductive sustainment of spheromaks* are not at hand, although there is experimental evidence that such spheromak sustainment has been achieved.[6,7] Instead, we invoke an extant simulation tool for the reversed field pinch (RFP), a close relative of the spheromak. In fact, the spheromak can be made to appear within the RFP itself by spatially modulating the RFP equilibrium, as will be described below.

The straight cylindrical version of the RFP is comprised of a set of axisymmetric magnetic fields and current densities, with both axial and azimuthal components. The characteristic RFP profile exhibits a reversal in the axial magnetic field profile, $B_z(r)$, as indicated in the upper half of Fig. 3. Magnetic fusion energy research on this magnetoplasma configuration was originally motivated by the experimental observation on a large-aspect-ratio toroidal discharge that fluctuations were dramatically reduced in the presence of the reversal, and a theoretical explanation was found to the effect that field-reconnecting MHD edge modes (double-tearing modes) were suppressed because the pitch profile of the field lines becomes monotonic in the presence of the reversal (assuming a cold edge region to be present). It was also shown that for sufficiently large axial currents, the presence of reversal in $B_z(r)$ signifies that the configuration is close to a state of minimum magnetic energy.[8]

However, the mechanism for steady sustainment of the reversed profile, observed in later experiments, was not made clear for some time, because the application of a voltage in the axial direction (inductively applied in the case of a large-aspect- ratio torus) has no obvious way to drive the necessary azimuthal currents along the purely azimuthal magnetic field at the reversal point. The reversal structure, therefore, ought to evolve away on a resistive time scale. The same difficulty persists in the case of spheromaks, which are visible as the 'o-points' in the lower half of Fig. 3. (The azimuthal direction in straight-cylindrical RFP geometry now becomes the toroidal direction of the spheromaks.)

Investigations into dynamo theory,[9] coupled with 3D resistive MHD simulations and some experimental confirmation gradually yielded some understanding of the situation. The resistive breaking of axisymmetry caused by global MHD instabilities (symptoms of the magnetoplasma trying to fall into a state of lower magnetic energy) brings into play a second order Lorentz electric field $\delta V \times \delta B$ that contains an axisymmetric component able to drive currents that are inaccessible to the axially applied voltage.

Here, the DEBS code[13,14] is applied to time-dependent simulations of a sustained, highly resistive, straight-cylindrical RFP, with energy and magnetic helicity supplied by an axial voltage. This code is pseudospectral

in space and semi-implicit in time. We ask whether the simulation will settle down into a steady state containing the axial-field reversal, albeit with altered symmetry. The applied voltage is continually adjusted during the simulation so as to maintain a constant total current. This voltage would be applied inductively for a truly toroidal RFP, but for a finite length segment it would be applied by external electrodes, as in spheromak experiments.[6,7] The axial periodicity length L_z is represented here as $L_z = 2\pi R_z$, where R_z is a pretend major radius of a torus so that the axial periodicity length is a pretend toroidal circumference for the straight model of the RFP. In the present simulation, unit aspect ratio is chosen, $R_z = a$, where a is the radius of the conducting wall of the cylinder (the minor radius in toroidal geometry). The code variables are normalized so that the initial value of magnetic field on axis is the unit of field, the cylinder radius is the unit of length, the resistive time, a^2/D, is the unit of time, but the initial Alfven velocity V_A on axis is the unit of velocity. The initial magnetic field profiles are depicted in Fig. 4, where the tokamak-type safety factor q (which is also the magnetic pitch profile normalized to $2\pi R_z$) is defined by $q = rB_z / R_z B_\theta$. (For the tokamak q would be greater than 1 at $r = 0$ and would rise to 3 or 4 at $r = a$.) For these simulations, the resistivity profile is taken to be uniform as is the plasma density.

As mentioned earlier, Lundquist numbers of order 10^6 and higher are of interest for magnetic fusion energy. Therefore, MHD simulationists in this area of research usually aspire to achieve the high spatial resolution needed to represent thin resistive tearing layers allowed by these large values of S. In the case of a gas core fission plasma, however, we are dealing with highly resistive plasmas, so new dynamo simulation runs were performed with S starting at 10^4 and going down. It was found that the RFP could be sustained in steady state by the dynamo activity for S as low as 200. It remains to be seen whether profile adjustments and the utilization of larger aspect ratios (which would support more MHD modes) can further drop this value. Results for S of 200 are shown in Figs. 5 and 6. Plots of the energy spectrum of fluctuations in Fig. 5 show that the state at 0.9 resistive times is helical, primarily containing poloidal mode number $m = 1$ and "toroidal" mode number $n = -2$. The steady resistive helical state has axisymmetric profile components ($m = 0$, $n = 0$) that are only moderately changed from the assumed initial zero-order state. The final q profile is seen to peak at 0.5 on the axis, showing that the dominant helical mode is resonant; that is, $q(0) = -m/n$. This condition of resonance signifies that the magnetic field lines need not be bent very much in order to participate in the growth (and saturation) of this mode. The plot of voltage vs time in Fig. 6-c shows that a steady state is reached well before one resistive time.

It is of interest to estimate physical magnitudes of some quantities from the simulation. Based on the normalizations specified above, the unit of axial applied voltage is

$$Voltage_{unit} = 2\pi (R_z / a) B_0 D$$

For an aspect ratio of 1, a field strength of 0.1 T, and a temperature slightly below 2 eV (for which the average charge state of pure uranium plasma at 1000 atm[5,10] is about 1 and the resistive diffusivity is $D \approx 100$ m^2/s), this expression yields about 50 volts for the unit of applied voltage in the code. [In ref. (5), D was erroneously too large, given as 1000 m^2/s for these parameters. For higher temperatures in pure uranium plasma D would be reduced by $T^{3/2}$, but would be increased by the increase of the mean ionic charge with temperature $Z(T)$. These two effects partially cancell one another.] This unit of voltage would have to be multiplied by the appropriate normalized number in the voltage plot in Fig. 6-c in order to give the physical applied voltage. The Lundquist number of 200 proves to be not quite appropriate for the gas core reactor, so that multiplication by the code voltage result of 20 to get 1 kV would be misleading.

Another quantity of interest here is the initial Alfven velocity on axis, which is the velocity unit used in the code. For an atmospheric-type uranium density of 2 10^{19} cm^{-3} and a field of 0.1 T, one finds $V_A \approx 35$ m/s. The kinetic energy spectrum for the $m = 1$ mode shown in Fig. 5 suggests a code velocity of 0.01 in association with this mode; but, again, this result of 0.3 m/s using the inappropriate Lundquist number would be misleading. Such dynamo flows could have an important influence on the disposition of the fuel plasma, and might even be used to advantage. Their patterns and magnitudes would have to be obtained from 3D resistive MHD simulations and examined using relevant input parameters in order to elucidate their effects on the fuel in gas core fission reactors.

The relevance of the RFP simulations to the spheromak is that the reversal surface of the RFP is susceptible to the formation of flux surface 'o-points' (magnetic islands) when the translational symmetry is broken by externally imposing an axially periodic modulation of the RFP equilibrium[15,16] (using bumpy conducting walls or an array of external coils), as shown in the lower half of Fig. 3. Each o-point structure is actually a spheromak, and is subject to resistive decay unless the axisymmetry is broken by saturated MHD instabilities providing dynamo activity, as alluded to earlier. This is because an axisymmetric steady state of the spheromaks cannot be maintained non-inductively with a voltage applied axially along the open field lines.

Now, instead of imposing axially periodic modulations of the RFP equilibrium, one may apply a set of aperiodic boundary conditions that effectively single out one axial segment that contains a single spheromak. This is known as the flux core spheromak[17] and its ideal equilibrium and stability properties have been studied theoretically. Since the supporting voltage is applied axially along the open field lines, the flux core spheromak again requires symmetry-breaking MHD modes to drive currents in the azimuthal direction, the toroidal direction of the spheromak.

Lundquist Numbers for Gas-Core Fission Plasmas

In this section, we shall present two examples of Lundquist numbers that might be achievable in gas core fission plasmas utilizing the gas-core parameter values described earlier. The examples are constrained by the power dissipated in the spheromak,[5] although this power would not be altogether lost but would be eventually absorbed in the propellant or the wall coolant.

The first case we consider is one in which the uranium core is diluted with lithium. Two advantages are that the lower mass density serves to increase the Alfven speed; and, the presence of lithium lowers the average ionic charge thereby increasing the electrical conductivity of the plasma. Both of these variations would increase S. A disadvantage is that the reduction in uranium number density implies a reduced opacity of the core. (The opacity of the lithium component is negligible.[12])

Elementary considerations of electrical conductivity of a mixture show that the mean ionic charge is effectively given by

$$Z = \frac{n_l Z_l^2 + n_u Z_u^2}{n_l Z_l + n_u Z_u} \qquad (6$$

wherein n and Z refer respectively to local number density and charge state, and l and u label the lithium and uranium species respectively. In the parameter range of interest here, $Z_l \approx 1$ and $Z_u \approx 3$, so that to bring Z down near 1 the lithium number density should exceed that of the uranium by at least a factor 30. Therefore we shall assume $n_u \approx 1\ 10^{18}$ cm^{-3} and $n_l \approx 3\ 10^{19}$ cm^{-3}. The presence of the lithium component also tends to maintain the core pressure near 1000 atm in spite of the reduced density of uranium.

According to the remarks made earlier, the core temperature is a consequence of the balance between the reactor power generation and the transport of thermal radiation outward through the opaque uranium, regardless of the presence of lithium (which has negligible opacity). In the present example this balance leads to a temperature of about 4 eV. Utilization of the Braginskii form of the Spitzer resistivity,[18] and including the effect of the mean ionic charge in Eq. (6), we obtain a resistive diffusivity of $D \approx 20$ m^2/s. The mass density of the core proves to be about 0.8 kg/m^3, so that the Alfven velocity is $V_A \approx 10^3\ B$ m/s, where B is a representative magnetic field strength in tesla. For a cylinder radius R of 4 meters, these inputs yield a Lundquist number

$$S \approx 200\ B$$

The attainment of sizeable Lundquist numbers from large fields, however, is constrained by the resistive (and dynamo) power dissipated in the spheromak. In ref. (5), an expression was derived giving the order of magnitude of the resistive power dissipated by a pressure-gradient-free spheromak as

$$P_{sph} = (4D)(\lambda R)^2 (B^2 / \mu_0) R$$

wherein λ is the force-free parameter and $(\lambda R)^2 \approx 10$ is characteristic of spheromak equilibria. For the considered parameters, this reduces to $P_{sph} \approx 0.3\ 10^{10} B^2$ watts. Thus, the magnetic field strength has to be limited to keep the power bounded, and this constraint also limits the size of S. For $B \approx 0.5$ T, one thereby finds $S \approx 100$ and $P_{sph} \approx 0.75$ GW. (The power needed to run the dynamo also would have to be taken into account in a more complete treatment of this problem.)

The second case we consider is one in which the uranium core is undiluted. We take a core number density of about $2\ 10^{19}$ cm^{-3} for which we earler estimated a core temperature of about 6 eV. For a mean ionic charge of about 3, we find $D \approx 29$ m^2/s, which is 1.5 times larger resistivity than the lithium case. The Alfven speed is now $V_A \approx 300\ B$ m/s, a factor of 3 worse than for the lithium case. The Lundquist number now becomes

$$S \approx 40\ B$$

where B is in tesla. The power dissipated in the spheromak is larger by the factor that D is larger, and we have $P_{sph} \approx 0.45\ 10^{10} B^2$ W. For $B = 0.5$ T, we obtain $S \approx 20$ and $P_{sph} \approx 1.1$ GW. (A reactor power level of 10 GW has been assumed.) Thus, diluting the core with lithium appears to better approach the goal.

Summary and Concluding Remarks

Putting aside, for now, considerations of specific space missions or of specific power-plant thruster system designs, we have investigated conditions under which gas-core fission criticality may be compatible with non-inductive sustainment of a spheromak plasma core. This investigation was along the following lines.

The neutronics, criticality properties, and heat transfer properties of gas core fission plasmas for the purpose of nuclear thermal propulsion were overviewed for parameter regimes conducive to achieving large Lundquist numbers in spite of these plasmas being highly resistive. Sufficiently large Lundquist numbers would open the possibility to utilize certain magnetoplasma configurations known in magnetic fusion energy research, so as to provide an additional means to beneficially influence the behavior of the fuel plasma. In the course of this overview, an analytic expression for the core temperature was derived, illustrating that the core temperature does not have a strong dependence on system parameters such as reactor power. The core temperature plays a crucial role in determining the plasma resistivity and hence the size of the Lundquist number. Also, it was pointed out that the moderately larger dimensions considered here [compared to those in ref. (1)] allow thicker propellant and neutron-moderator layers such that higher propellant temperatures and higher specific impulses may be attained; and, concomitantly, that the increased energy upscattering of thermal neutrons by the thicker hotter hydrogen propellant layer may be utilized with ^{233}U fuel to improve the criticality parameter k_{eff} over what it would be with ^{235}U. Criticalities near unity or slightly above were found to be feasible with the larger dimensions and thicker propellant and moderator layers in conjunction with the utilization of ^{233}U fuel.

These parameters from un-optimized configurations then were input to sample calculations of the Lundquist number S in fission core plasmas. Also, un-optimized 3D MHD simulations were performed indicating the smallest values of S for which non-inductive sustainment of reversed field pinches (and presumably spheromaks), by the dynamo activity of helical MHD instabilities, appeared to be possible. Surprisingly, dynamo sustainment was found to exist for S down to 200 for unit aspect ratio. Also surprisingly, S values substantially larger than unity were estimated for fission core plasmas, S values up to 100. The dilution of

the uranium core with ^{7}Li proved to be a superior method to just working with a pure uranium core, in spite of the reduction in plasma opacity.

Whether the value of 100 can be reasonably increased, and the value of 200 can be reasonably decreased, is a question that has to be answered by optimization studies. Even if such a matching of S values could be attained, there remains the critical question of the influence of the plasma dynamo flows on the disposition of the fuel, and whether such flows might be used to advantage.

Acknowledgements

One of the authors (RG) benefitted from discussions with Los Alamos colleagues J. M. Finn, J. J. Keady, and N. H. Magee.

References

[1] Poston, D. I., "A Computational Model for an Open Cycle Gas Core Nuclear Rocket," Ph. D. Dissertation, Dept. of Nuclear Engineering, Univ. of Michigan, Ann Arbor, June 1994.

[2] Poston, D. I., and Kammash, T., "Hydrodynamic Fuel Containment in an Open-Cycle Gas-Core Nuclear Rocket," Proceedings of the 11*th* Symposium on Space Nuclear Power Systems, Albuquerque, NM, Jan. 1994, American Institute of Physics ISBN # 1-56396-305-1 AIC Conference Proceedings # 301, p1415.

[3] Poston, D. I., and Kammash, T., "A Comprehensive Thermal-Hydraulic Model of an Open-Cycle Gas-Core Nuclear Rocket," *ibid*, p473.

[4] Poston, D. I., and Kammash, T., "A Neutronic Study of the Open-Cycle Gas-Core Nuclear Rocket," AIAA-94-2896, Proceedings of the 30*th* AIAA/ASME/SAE/ASEE Joint Propulsion Conference, Indianapolis, IN, June 1994.

[5] Gerwin, R. A., "Magnetic Control of Fission Plasmas," AIAA 94-3267, *ibid*.

[6] Jarboe, T. R., Barnes, C. W., Platts, D. A., and Wright, B. L., "A Kinked Z-Pinch as the Helicity Source for Spheromak Generation and Sustainment," *Comments on Plasma Physics and Controlled Fusion*, Vol. IX, No. 4, 1985, p161.

[7] Fernandez, J. C., Wright, B. L., Marklin, G. J., Platts, D. A., and Jarboe, T. R., "The m=1 Helicity Source Spheromak Experiment," *Physics of Fluids*, Vol. B1, June 1989, p1254.

[8] Taylor, J. B., "Relaxation and Magnetic Reconnection in Plasmas," *Reviews of Modern Physics*, Vol. 58, No. 3, 1986, p741.

[9-a] Aydemir, A., Barnes, D., Caramana, E. J., Mirin, A., Nebel, R. A., Schnack, D. D., and Sgro, A. G., "Compressibility as a Feature of Field Reversed Maintenance in the Reversed Field Pinch," *Physics of Fluids*, Vol. 28, March 1985, p898. [9-b] Finn, J. M., Nebel, R. A., and Bathke, C., "Single and Multiple Helicity Ohmic States in Reversed Field Pinches," *Physics of Fluids*, Vol. B4, May 1992, p1262.

[10] Parks, D. E., Lane,G., Stewart, J. C., and Peyton, S., "Optical Constants of Uranium Plasma," Gulf General Atomic Rept. GA-8244, NASA CR-72348, Feb. 1968.

[11] Briesmeister, J. F., "MCNP - A General Monte Carlo N-Particle Transport Code," Los Alamos National Laboratory Rept. LA-12625-M, 1993.

[12] Keady, J. J., and Magee, N. H., Los Alamos National Laboratory Atomic Physics Theory Group, priv. comm.

[13] Schnack, D. D., Barnes, D. C., Mikic, Z., Harned, D. S., and Caramana, E. J., "Semi-implicit magnetohydrodynamic calculations," *J. Comput. Physics*, Vol. 70, 1987, p330.

[14] Schnack, D. D., Barnes, D. C., Mikic, Z., Harned, D. S., Caramana, E. J., and Nebel, R. A., "Numerical Simulation of Reversed Field Pinch Dynamics," *Comput. Physics. Comm.*, Vol. 43, 1986, p17.

[15] Jensen T. H., and Chu, M. S., "The Bumpy Z-Pinch," *J. Plas. Physics*, Vol. 25, 1981, p459.

[16] Chu, M. S., Jensen, T. H., and Dy, B., "Method for finding minimum energy three-dimensional magnetohydrodynamic equilibria with given constraints," *Physics of Fluids*, Vol. 25, 1982, p1611.

[17] Finn, J. M., and Guzdar, P. N., "Formation of a Flux Core Spheromak," *Physics of Fluids*, Vol. B3, April 1991, p1041.

[18] Braginskii, S. I., "Transport Processes in a Plasma," in Reviews of Plasma Physics, Vol. 1, Consultants Bureau, New York, 1965, p205.

List of Figures

Fig. 1 Examples of gas-core open-cycle fission reactor.

a) Schematic of straightforward cylindrical concept, with propellant and fuel (injected at left) heated by fission power density p_f. Heated propellant is blown out through nozzle at right.

b) Schematic of spheromak approach showing pellet-injected core of ^{233}U in toroidal volume of closed magnetic flux surfaces, surrounded by a layer of flowing hydrogen propellant and a layer of moderator.

Fig. 2 Rosseland absorption constant in m^{-1} *vs* temperature in K for pure uranium at 1000 atm.

Fig. 3 Reversed field pinch configuration showing axially modulated equilibrium in lower half.

Fig. 4 Initial magnetic field profiles for simulation with unit aspect ratio and $S = 200$.

a) Axial magnetic field $B_z(r/a)$.

b) Azimuthal magnetic field B_θ (r/a).

c) Safety factor or normalized pitch profile $q(r/a)$.

Fig. 5 Development of helical MHD modes in reversed field pinch at 0.9 resistive times.

a) Magnetic energy mode spectrum, showing dominant $m = 1, n = -2$ magnetic perturbation. (Other helicities possess much smaller energies.)

b) Kinetic energy mode spectrum, showing dominant flow field $m = 1, n = -2$ structure. (Other helicities possess much smaller energies.)

Fig. 6 Axisymmetric aspects of the helically deformed reversed field pinch.

a) Normalized pitch profile at 0.9 resistive times, showing resonance with dominant helical mode.

b) Paramagnetic inward pinch velocity, for which the resulting mass pile-up would be averted by outward fluctuation-induced transport $< \delta\rho\ \delta V >$ in a more complete model. (The paramagnetic velocity would arise in the "flux core" open line region of the spheromak.)

c) Applied voltage (continually adjusted so as to maintain constant current) *vs* time, illustrating a rapid approach to a steady state within one resistive time.

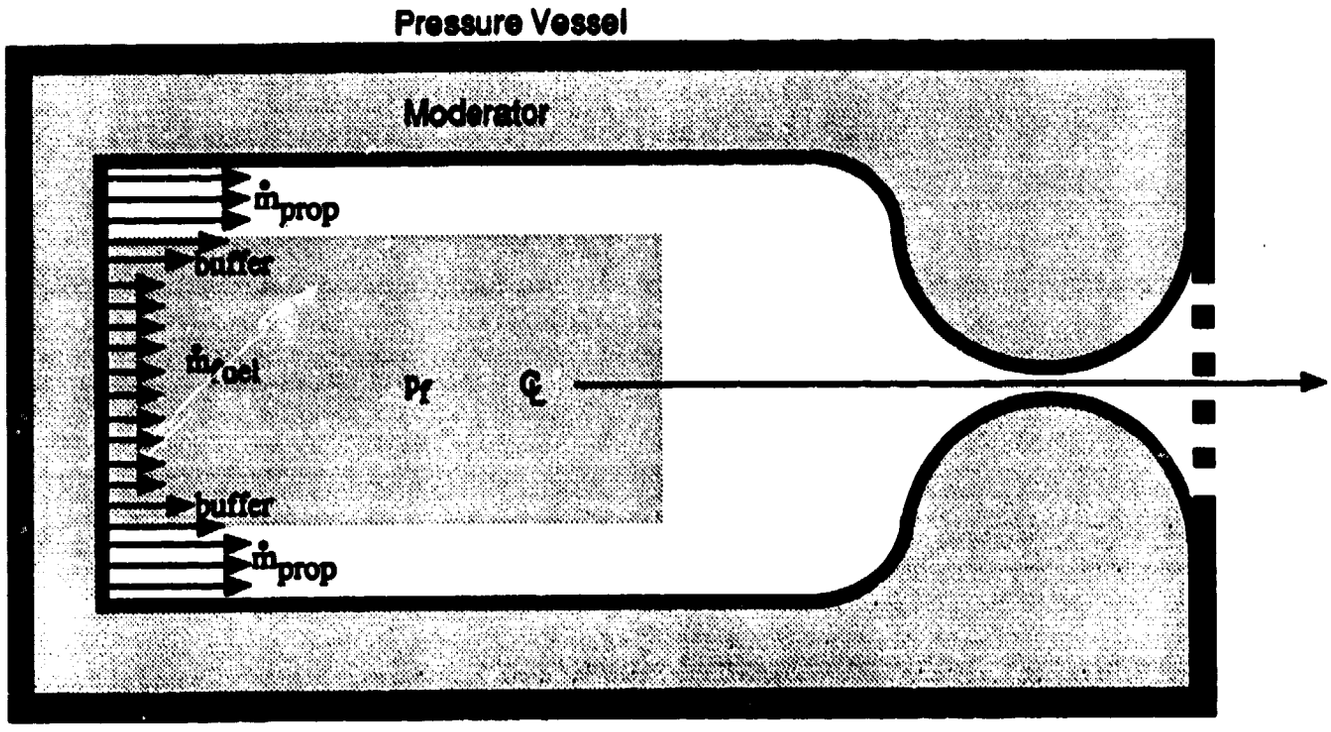
Pressure Vessel
Moderator
$\dot{m}_{prop}$
buffer
$\dot{m}_{fuel}$
P_f
$\mathcal{C}_L$
buffer
$\dot{m}_{prop}$

Fig. 1-a

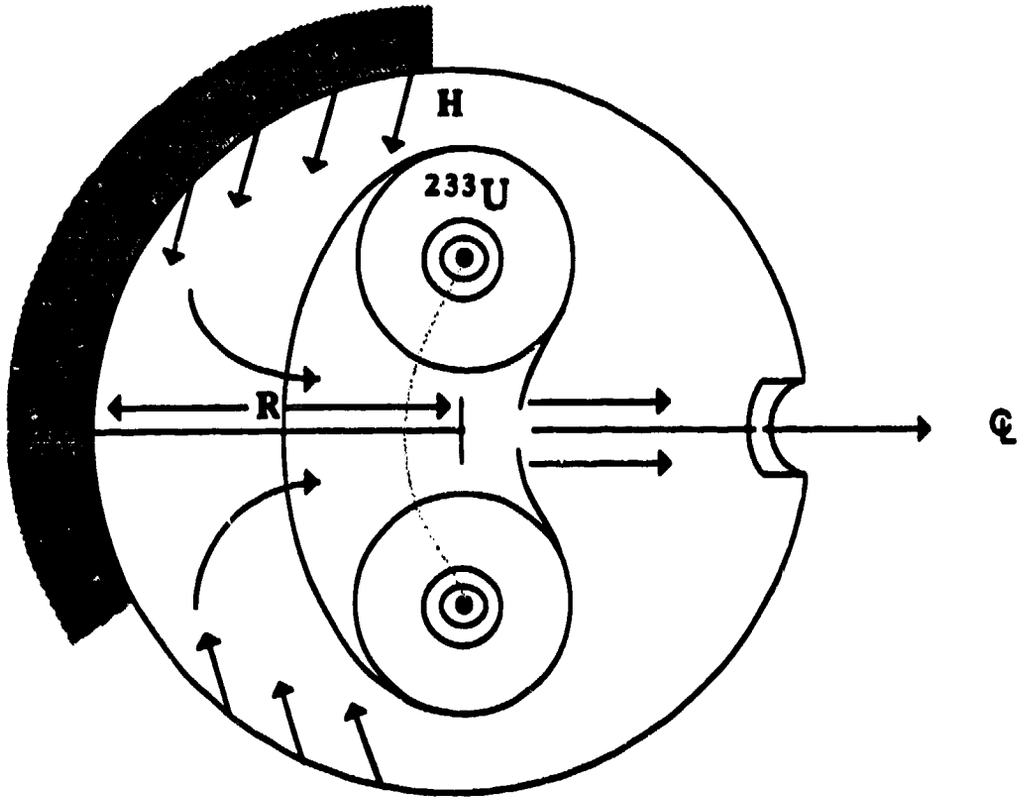
H
^{233}U
R
$\mathcal{C}_L$

Fig. 1-b

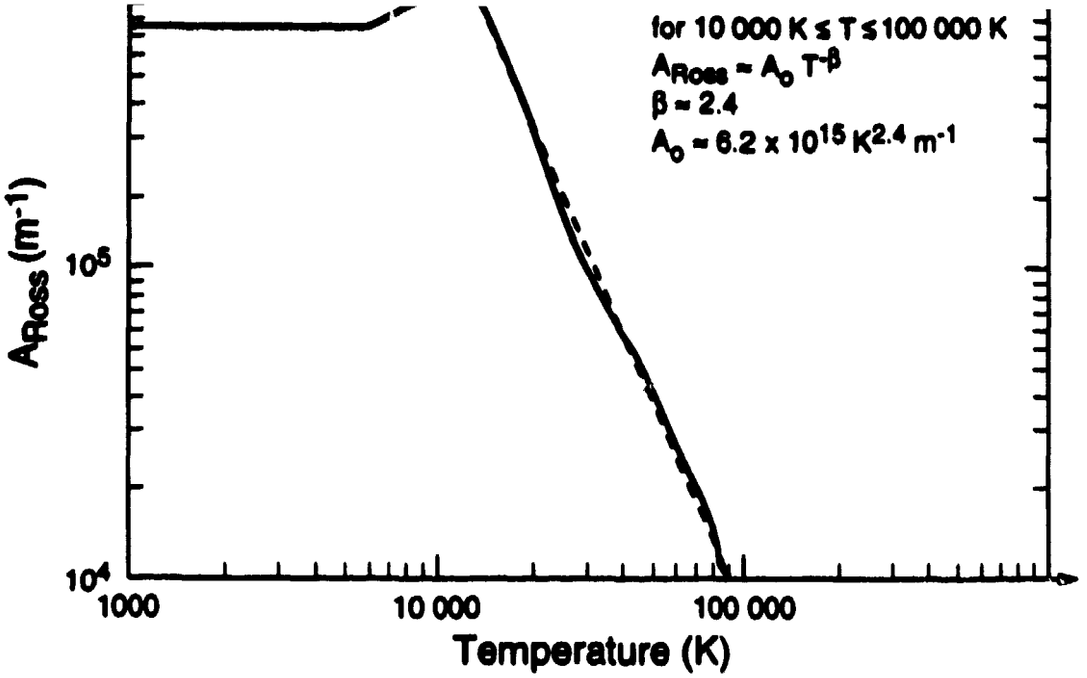
for 10 000 K ≤ T ≤ 100 000 K
$A_{Ross} = A_0 T^{-\beta}$
$\beta = 2.4$
$A_0 = 6.2 \times 10^{15}\ K^{2.4}\ m^{-1}$
$A_{Ross}\ (m^{-1})$
10^5
10^4
1000
10 000
100 000
Temperature (K)

Fig. 2

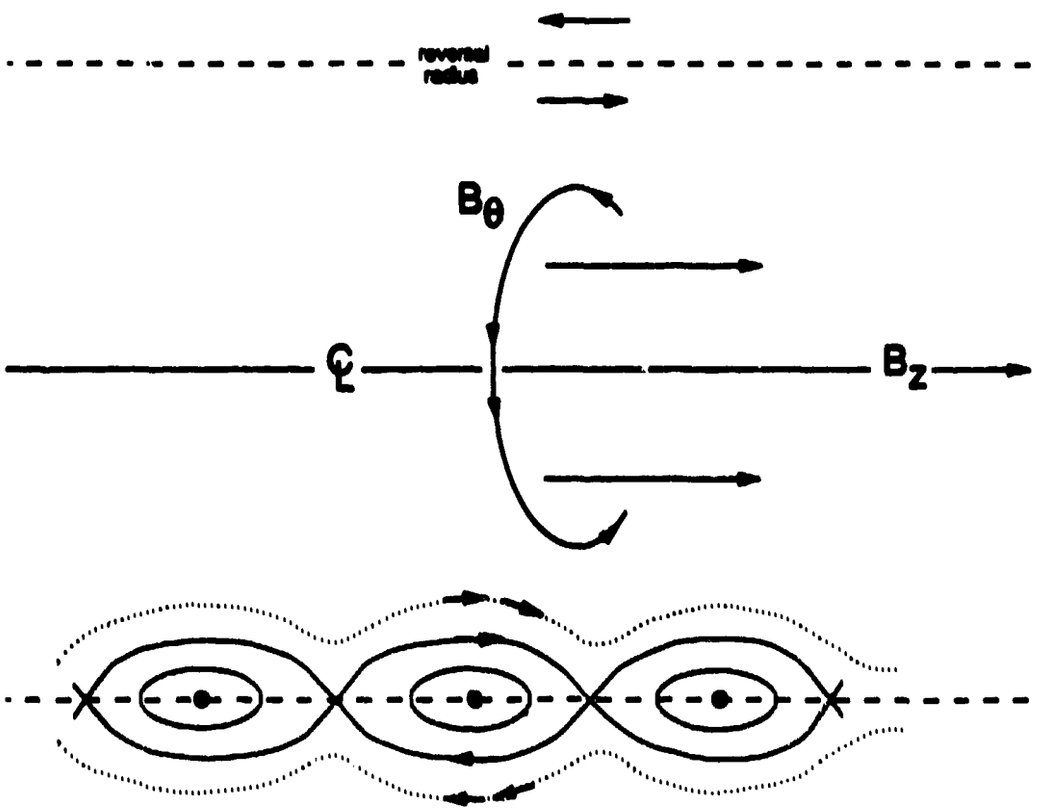
reversal radius
B_θ
B_z

Fig. 3

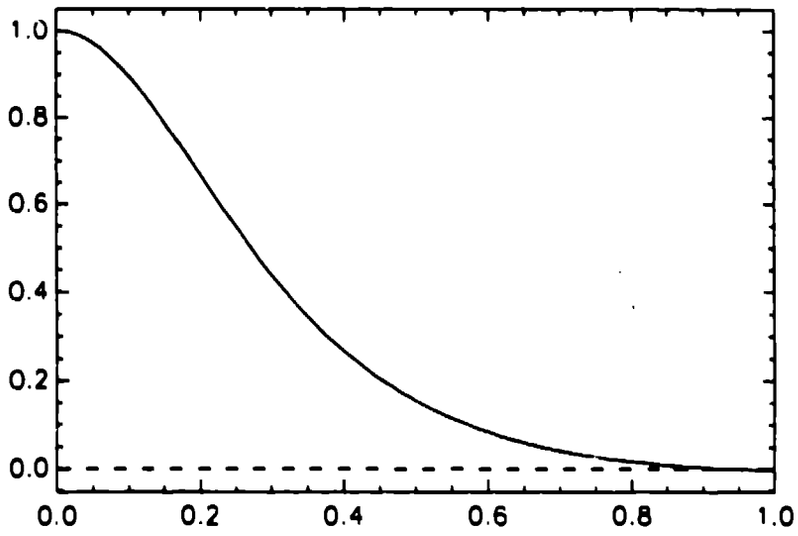

Fig. 4-a

theta magnetic field m= 0 n= 0

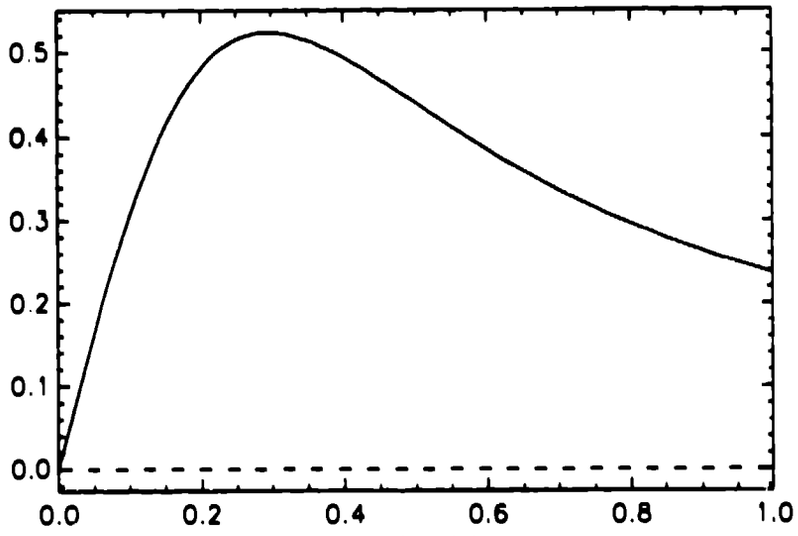

Fig. 4-b

safety factor m= 0 n= 0

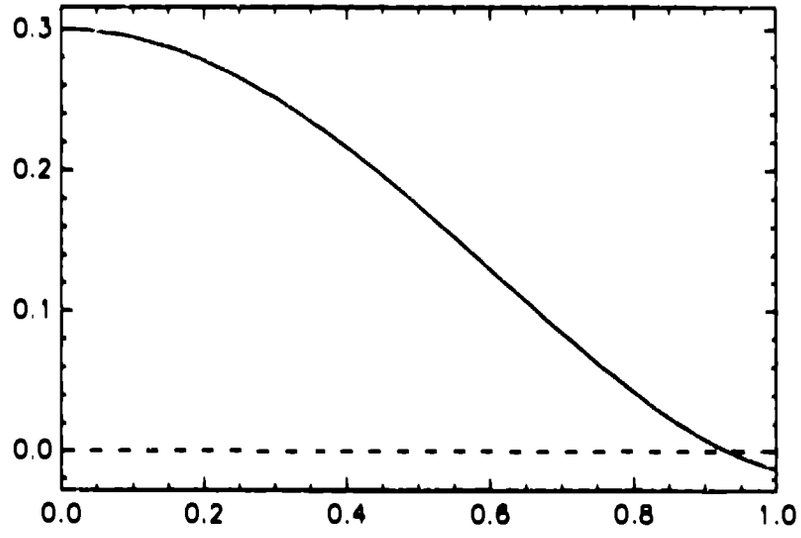

Fig. 4-c

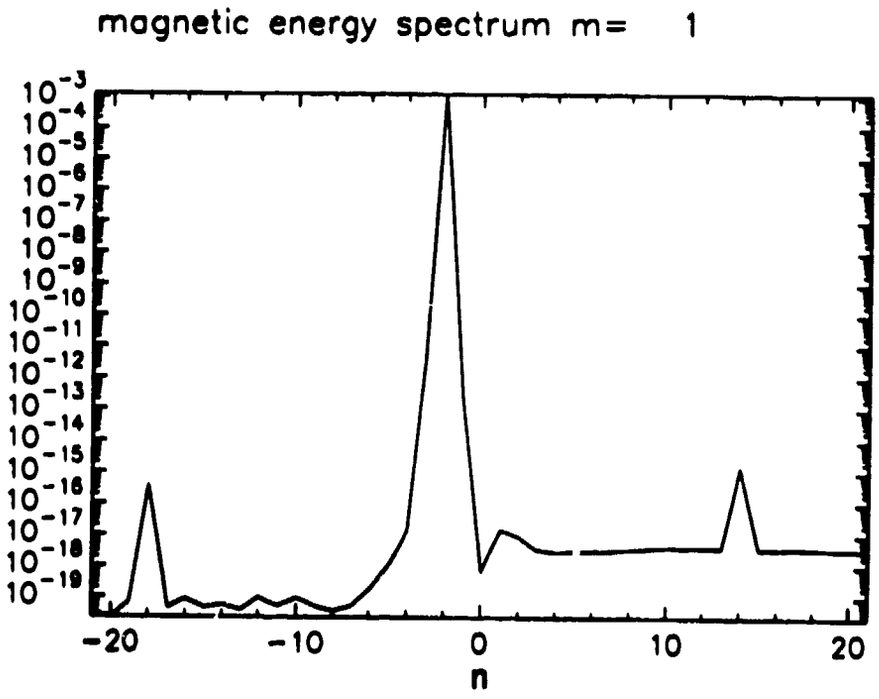
magnetic energy spectrum m= 1
10^-3
10^-4
10^-5
10^-6
10^-7
10^-8
10^-9
10^-10
10^-11
10^-12
10^-13
10^-14
10^-15
10^-16
10^-17
10^-18
10^-19
-20
-10
0
10
20
n

Fig. 5-a

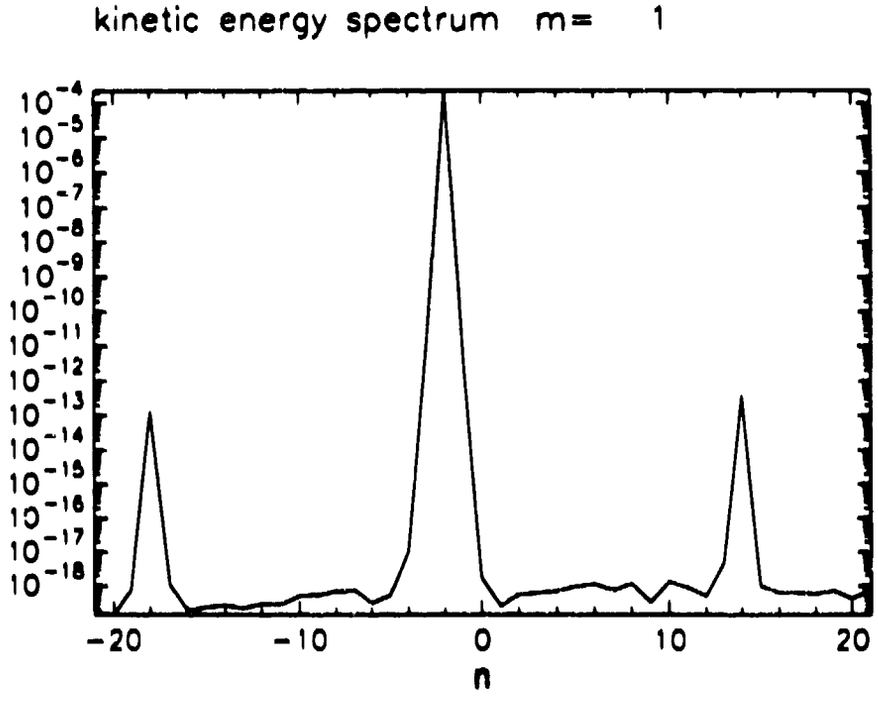
kinetic energy spectrum m= 1
10^-4
10^-5
10^-6
10^-7
10^-8
10^-9
10^-10
10^-11
10^-12
10^-13
10^-14
10^-15
10^-16
10^-17
10^-18
-20
-10
0
10
20
n

Fig. 5-b

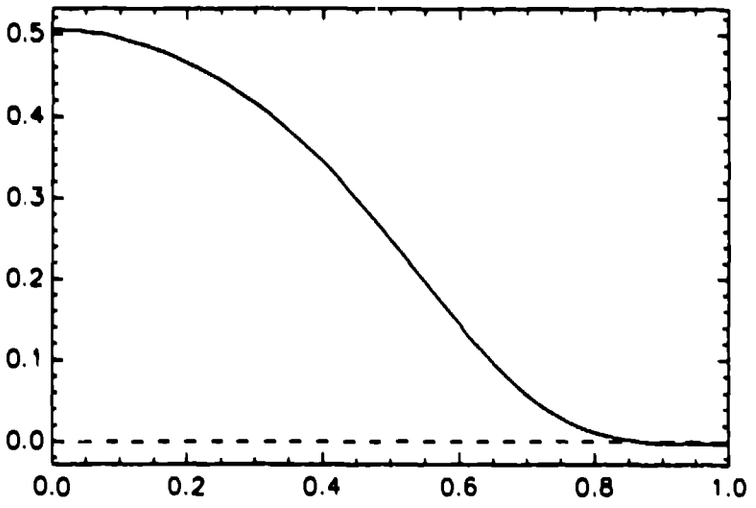

Fig. 6-a

radial velocity m= 0 n= 0

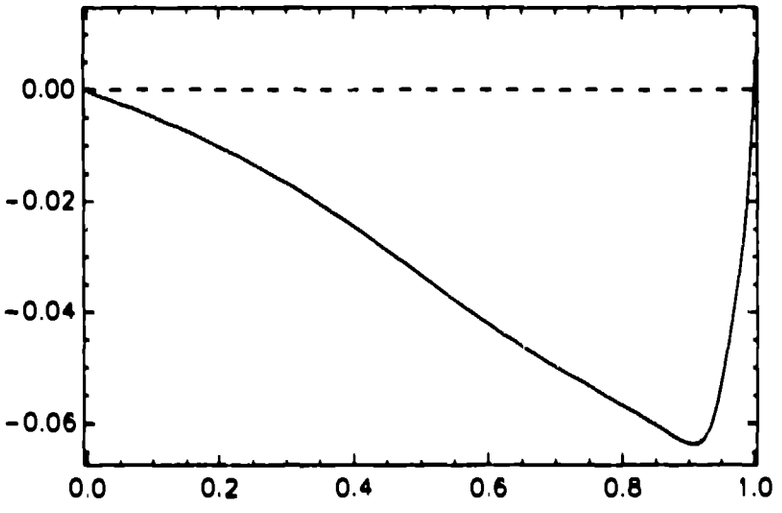

Fig. 6-b

tor. voltage vs. time

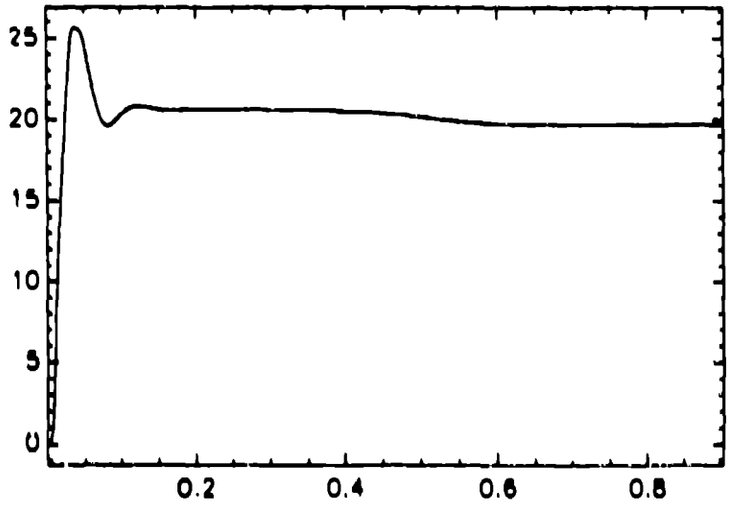

Fig. 6-c